

**SeaWiFS vicarious calibration: an alternative approach which makes use of simultaneous *in situ* observations of oceanic and atmospheric optical properties.**

Bryan A. Franz, Ewa Ainsworth  
*SAIC General Sciences Corporation, Beltsville, Maryland*

Sean Baily  
*Futuretech Corporation, Greenbelt, Maryland*

Abstract

A technique was developed which makes use of simultaneous measurements of *in situ* water-leaving radiance and aerosol optical thickness to derive a vicarious calibration for the eight SeaWiFS wavelengths. In this chapter, we briefly review the atmospheric radiative transfer model and the standard technique used to calibrate the SeaWiFS instrument through *in situ* water-leaving radiance measurements. We then build on that standard approach using additional information from *in situ* atmospheric observations to reduce the number of required assumptions. We apply this revised technique to derive a new calibration for SeaWiFS, and compare results with the operational calibration.

## 9.1 INTRODUCTION

We will first describe an approach for estimating the top-of-atmosphere (TOA) reflectance using simultaneous measurements of *in situ* water-leaving radiance and aerosol optical thickness at the SeaWiFS wavelengths. This approach can be used to predict the radiance that should be observed in each of the eight SeaWiFS bands, thereby providing a mechanism for direct calibration of the sensor. We apply this technique to the vicarious calibration of SeaWiFS and contrast the results with those obtained for the operational SeaWiFS calibration, through comparison with independent *in situ* measurements of water-leaving radiances and aerosol optical thickness.

## 9.2 ALGORITHM DESCRIPTION

We begin with the definition of the reflectance,  $\rho = \pi L / \mu_0 F_0$ , where  $L$  is the radiance in a given solar and viewing geometry,  $F_0$  is the extraterrestrial solar irradiance, and  $\mu_0$  is the cosine of the solar zenith angle. The total reflectance measured at the top of the ocean-atmosphere system,  $\rho_t(\lambda)$ , can be written as:

$$\rho_t(\lambda) = [\rho_r(\lambda) + \rho_a(\lambda) + \rho_{ra}(\lambda) + T(\lambda)\rho_g(\lambda) + t(\lambda)\rho_f(\lambda) + t(\lambda)\rho_w(\lambda)]t_g(\lambda), \quad (1)$$

where  $\rho_r(\lambda)$  is the reflectance resulting from multiple scattering by air molecules in the absence of aerosols,  $\rho_a(\lambda)$  is the reflectance resulting from multiple scattering by aerosols in the absence of air molecules,  $\rho_{ra}(\lambda)$  is the multiple interaction term between molecules and aerosols [1],  $\rho_g(\lambda)$  is the direct reflectance of solar rays from the sea surface to the sensor (Sun glint or glitter),  $\rho_f(\lambda)$  is the reflectance at the sea surface that arises from sunlight and skylight reflecting from whitecaps on the surface [2], and  $\rho_w(\lambda)$  is the water-leaving reflectance, which is the desired quantity in ocean color remote sensing. The  $t(\lambda)$  term is the atmospheric diffuse transmittance [3] that accounts for the effects of propagating a diffuse light source from the sea surface to the TOA. Similarly,  $T(\lambda)$  is the direct transmittance which accounts for the effects of propagating a beam of light from the sea surface to the TOA. The  $t_g(\lambda)$  term represents the gaseous transmittance, which accounts for absorption due to ozone, oxygen, and water vapor.

The calibration process involves computing the TOA reflectance from known and measured components of Equation 1, and comparing the predicted value with the observed value from SeaWiFS to derive a calibration gain and possibly an offset. In practice, the molecular scattering signal is well understood and can be accurately computed [7]. The white cap signal is generally small, and it can be predicted using statistical relationships and ancillary wind speed data [18]. Furthermore, the residual uncertainties can be minimized by using observations with low surface wind speeds. The Sun glint term can be predicted from solar and viewing geometry and ancillary wind field

data [17], but in practice it is easily avoided by limiting observations to geometries which do not allow for direct reflectance of the solar rays into the sensor. Avoiding Sun glint also alleviates the need to know the direct transmittance. The gaseous transmittance can be predicted from ancillary data on ozone and water vapor concentrations, solar and viewing geometries, and the spectral band passes of the sensor [4, 5, 6]. This leaves the water-leaving reflectances, aerosol and Rayleigh-aerosol terms, and the diffuse transmittance to be derived from *in situ* measurements or additional assumptions.

In practice, the water-leaving reflectance values at a given location can be derived from *in situ* optical measurements of the upwelling radiance. The remaining terms in Equation 1 require some knowledge or assumptions about the aerosol type and concentration. This includes the diffuse transmittance term, which is dominated by molecular scattering effects but is weakly influenced by the aerosols [3].

The standard approach used by the SeaWiFS project to account for the influence of aerosols in the vicarious calibration [8,15,16] has been to make two assumptions: 1) that the gain at 865nm is known and fixed at the pre-launch value, and 2) that the aerosol type near the calibration site is characterized by an average maritime model [15]. The first assumption essentially fixes the aerosol concentration, while the latter assumption determines the relative calibration between the 765 and 865nm channels and the extrapolation of aerosol reflectance to the visible bands. This has been the calibration technique employed for all SeaWiFS processing to date.

The focus of the present work is to develop a technique which eliminates or reduces the aerosol assumptions by making use of aerosol optical thickness measurements which have been collected in conjunction with *in situ* water-leaving radiances. What we require is a method to relate measurements of aerosol optical thickness to total multiple-scattering aerosol reflectance, including the effect of Rayleigh-aerosol interaction.

In the single-scattering approximation, the aerosol reflectance,  $\rho_{as}(\lambda)$ , can be computed as

$$\rho_{as}(\lambda) = \frac{\omega_0(\lambda) \tau_a(\lambda) P_a(\lambda, \Theta)}{4\mu_0\mu}, \quad (3)$$

where the subscript s denotes single-scattering. In Equation 3,  $\omega_0(\lambda)$  is the single-scattering aerosol albedo,  $\tau_a(\lambda)$  is the aerosol optical depth,  $P_a(\lambda, \Theta)$  is the scattering phase function for a scattering angle of  $\Theta$ , and  $\mu_0$  and  $\mu$  are the cosines of the solar and view zenith angles, respectively. The aerosol optical thickness at each wavelength can be obtained from available *in situ* measurements, but the single scattering albedo and scattering phase function require knowledge of the aerosol type.

A simple approach to characterize the aerosol type is to define the Ångström coefficient,  $\alpha(\lambda_1, \lambda_2)$ , as

$$\frac{\tau_a(\lambda_1)}{\tau_a(\lambda_2)} = \left(\frac{\lambda_1}{\lambda_2}\right)^{-\alpha}. \quad (4)$$

Using this characterization, we can compare the measured Ångström coefficient to the Ångström coefficients associated with a set of aerosol models, and from the models with similar Ångström coefficient we can retrieve the single-scattering albedo and scattering phase function. In general, the measured Ångström coefficient will fall between two of the models, so we compute Equation 3 for each model (call them  $\rho_{as1}(\lambda)$  and  $\rho_{as2}(\lambda)$ ) and we define a mixing ratio,  $R$ , to interpolate between the two models. Before we interpolate, however, we take advantage of the model relationships developed by Gordon and Wang [4] to translate the single-scattering aerosol reflectances for model  $i$  to multiple-scattering aerosol reflectance with Rayleigh-aerosol interaction,  $[\rho_a(\lambda) + \rho_{ar}(\lambda)]_i$ . Thus, we can now compute the total aerosol reflectance as

$$\rho_a(\lambda) + \rho_{ar}(\lambda) = R[\rho_a(\lambda) + \rho_{ar}(\lambda)]_1 + (1 - R)[\rho_a(\lambda) + \rho_{ar}(\lambda)]_2 \quad (5)$$

In a similar way, we can compute the Rayleigh-aerosol diffuse transmittance for each aerosol model [3] and interpolate to retrieve the total diffuse transmittance.

### 9.3 APPLICATION TO SEAWIFS CALIBRATION

The primary calibration site for the SeaWiFS project is the MOBY buoy [9], located off the coast of Lanai, Hawaii. Since 1996, the MOBY buoy has been continuously collecting upwelling radiance measurements at fine spectral resolution through the visible wavelength regime. MOBY measurements are collected for each satellite overpass, and processed to provide water-leaving radiances at each of the SeaWiFS visible band passes (412 – 670 nm). The water-leaving radiances in the two SeaWiFS near infrared (NIR) bands can be assumed to be negligible, or estimated from a case 1 model [10].

In 1998, the SIMBIOS Project began operating a Cimel sun photometer at Lanai as part of the Aerosol Robotic Network, AERONET [12,13,14]. This sun photometer measures aerosol optical thickness at seven wavelengths (340, 380, 440, 500, 670, 870, and 1020 nm). For these data to be useful as inputs for the calibration technique described herein, an estimate of the optical thickness at each of the SeaWiFS bands must be determined. To do this we apply a simple linear fit to  $\log(\tau_a)$  vs  $\log(\lambda)$ . Using this fit, we interpolate the  $\tau_a(\lambda)$  to the SeaWiFS nominal wavelengths. If the residuals from this linear fit are more than five percent of the measured value, the record is rejected.

We have identified 38 SeaWiFS scenes over MOBY for which there exist contemporaneous aerosol measurements at Lanai, and which pass the standard SeaWiFS exclusion criteria for vicarious calibration [16]. Additionally, measurement were excluded if the *in situ* measured  $\tau_a(865)$  was less than 0.02 or the wind speed was greater than 5 m/s. The threshold on  $\tau_a(865)$  was set to account for the uncertainty in the calibration of the Cimel aerosol optical thickness retrievals. The AERONET group reports an uncertainty of  $\pm 0.01$  in  $\tau_a(\lambda)$  [12]. The wind speed threshold was set to reduce uncertainties in the atmospheric correction algorithm, as the Rayleigh and whitecap radiances are both wind speed dependent. This left only 5 calibration points. Using the inversion technique described above on these 5 points, we have computed a set

of vicarious gains for all eight SeaWiFS bands. These alternative gains are listed with the operational gains for SeaWiFS reprocessing #3 in Table 1.

Table 1: *SeaWiFS vicarious gain coefficients, operational and alternative.*

Gain Type	Band 1	Band 2	Band 3	Band 4	Band 5	Band 6	Band 7	Band 8
Operational	1.00310	0.991158	0.959938	0.985839	0.993857	0.959650	0.946	1.0
Alternative	1.005726	0.995034	0.968053	0.989528	0.995204	0.953351	0.923352	0.955989

Table 2: *Statistical comparison of bio-optical match-up results for both operational and alternative vicarious gains.*

SeaWiFS Band	SeaWiFS :In situ Ratio	Std. Dev.	R-square	N
All Match-ups				
Alternative Vicarious Calibration Gains				
1	0.7135	0.3085	0.6478	209
2	0.9176	0.3040	0.7618	228
3	1.0203	0.2859	0.7514	233
4	1.0876	0.3140	0.7011	221
5	1.1278	0.3182	0.8387	233
Operational Vicarious Calibration Gains				
1	0.7929	0.3255	0.7175	192
2	0.9621	0.3333	0.7641	202
3	1.0122	0.2970	0.7559	207
4	1.0793	0.3275	0.5975	195
5	1.0993	0.3385	0.6952	207
Case 1 Match-ups				
Alternative Vicarious Calibration				
1	0.8273	0.1997	0.8218	118
2	0.9576	0.2296	0.8313	140
3	1.0140	0.2211	0.7575	157
4	1.0672	0.2338	0.4432	143
5	1.1031	0.2772	0.3822	146
Operational Vicarious Calibration				
1	0.8520	0.2146	0.8132	125
2	0.9628	0.2407	0.8282	145
3	0.9906	0.2171	0.7508	156
4	1.0403	0.2308	0.3392	143
5	1.0560	0.2697	0.3454	150

## 9.4 RESULTS AND DISCUSSION

As reproduced from Bailey et al. [11], the SeaWiFS bio-optical match-up results of Figure 1 were processed using the operational gains. A comparison of the coefficients in Table 1 would suggest that the assumption of unity for the gain in band 8 is an overestimate on the order of 5%. Overall the results of the match-ups with the alternative gains, as presented in Figure 2, show that bio-optical comparisons between *in situ* measurements and SeaWiFS derived values are not greatly affected by this change of calibration. A comparison of the statistics by band are found in Table 2. From the comparison of the alternative gains to the operational gains, we find a slight improvement in bands 4 and 5 and a slight degradation in the bio-optical match-up results for band 1 .

The results of AOT match-ups between *in situ* and SeaWiFS measurements indicate that the alternative vicarious gain coefficients can cause improvements in the outcome of SeaWiFS atmospheric correction in terms of AOT levels. This is because the alternative calibration method eliminates *a priori* assumptions on band 8 calibration and aerosol type over MOBY, which strongly influence aerosol determination in the SeaWiFS processing. Figure 3 shows the comparison of match-ups obtained using the operational gains, top two graphs, and the alternative gains, bottom two graphs. *In situ* AOT points were extracted using the statistical screening on the single CIMEL 870nm band (Chapter 6). Only the results in the 443nm and 865nm bands are displayed.

For the operational gains, the slope of a linear fit between both types of AOT observations is close to 1 in the 865nm band and the intercept indicates a small shift of 0.02 in the AOT value. The application of alternative gains causes the slope of the linear fit in the 865nm band to decrease, however, the intercept is the same and the overall inaccuracy of match-ups is reduced. For the alternative

gains, the large majority of AOT points are closely clustered along the  $y=x$  line and there are only a few outliers which adversely influence the statistics.

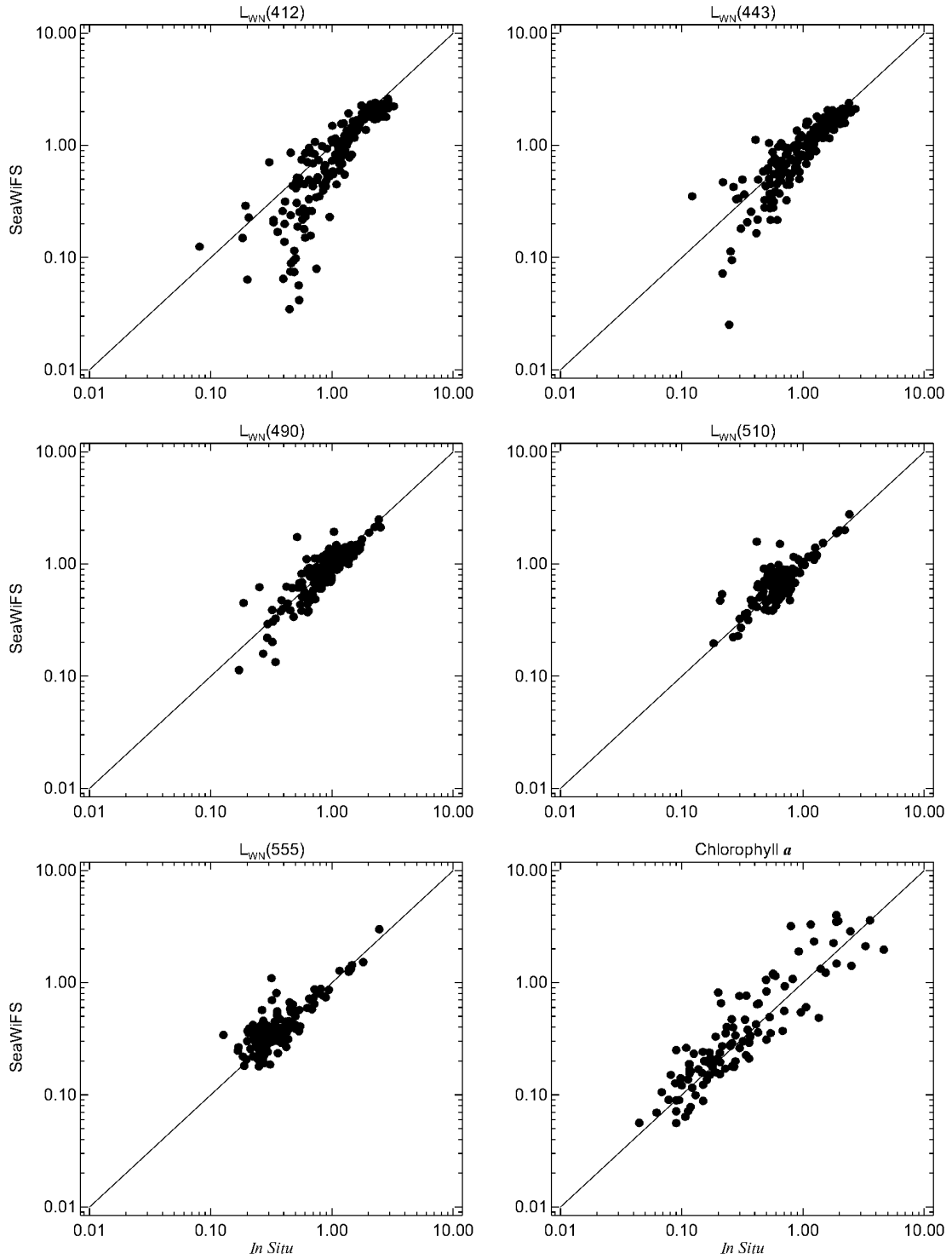


Figure 1: In situ comparison with SeaWiFS retrieved normalized water-leaving radiances when using operational vicarious gains.

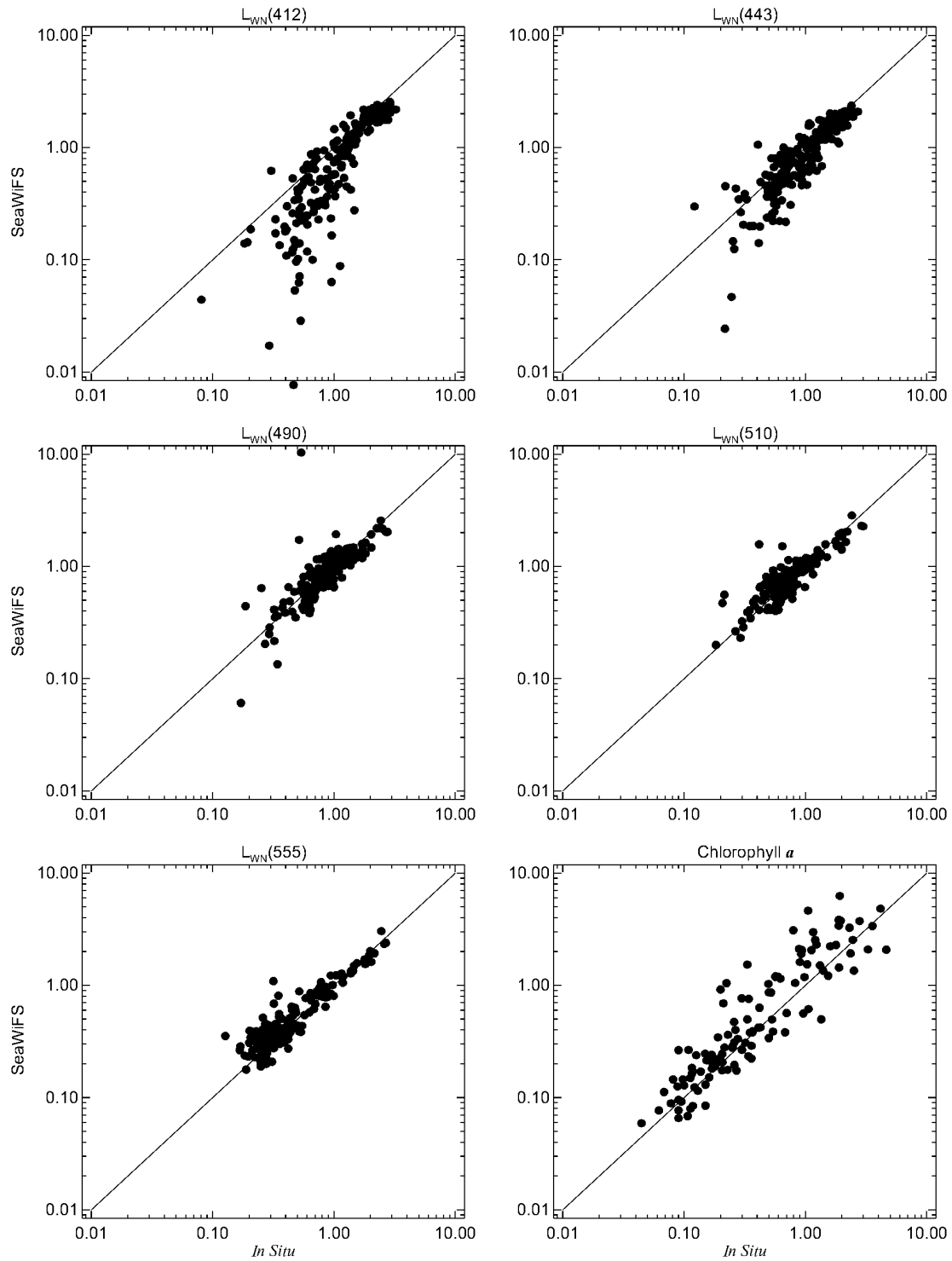


Figure 2: In situ comparisons to SeaWiFS retrieved water-leaving radiances when using alternative, AOT-based vicarious gains.

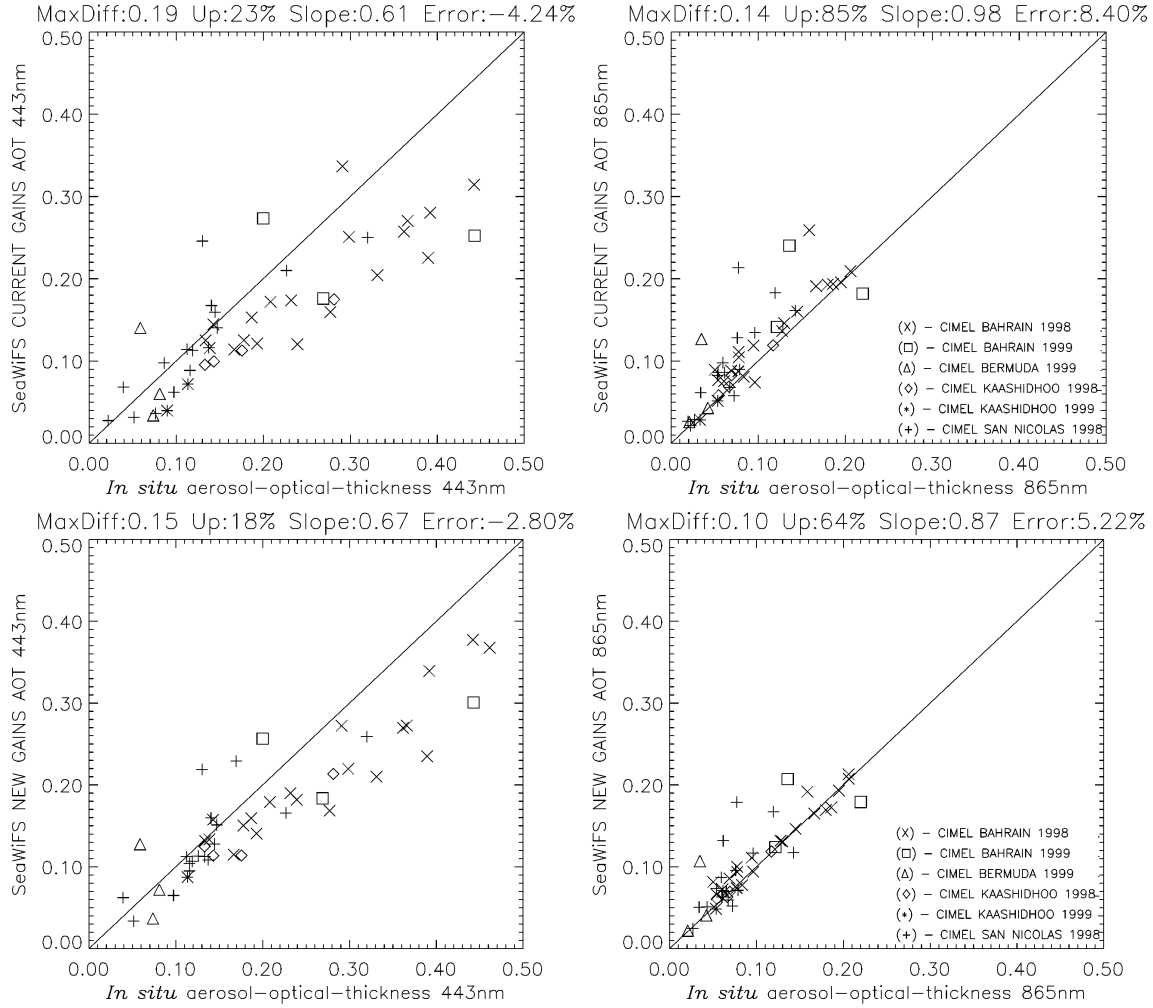


Figure 3. Comparison of AOT match-ups in the 443nm and 865nm bands for the operational and alternative set of SeaWiFS calibration gains.

The alternative SeaWiFS calibration method uses existing aerosol models to provide the estimate of the multi-scattering aerosol reflectance with Rayleigh-aerosol interaction. These aerosol models have been noticed before to exhibit AOT spectral distributions which are flatter than the AOT distributions obtained from *in situ* measurements (Chapter 7). Therefore, *in situ* AOT values are generally underestimated by the SeaWiFS algorithm in the shorter visible wavelengths. This underestimation is decreased but is still significant when the alternative calibration gains are applied in the SeaWiFS processing, as shown for the band at 443nm in Figure 3. In this band, the inaccuracy of the match-ups

is decreased somewhat with the application of the alternative gain set and the slope of the linear fit between *in situ* and SeaWiFS AOT measurements is only slightly improved.

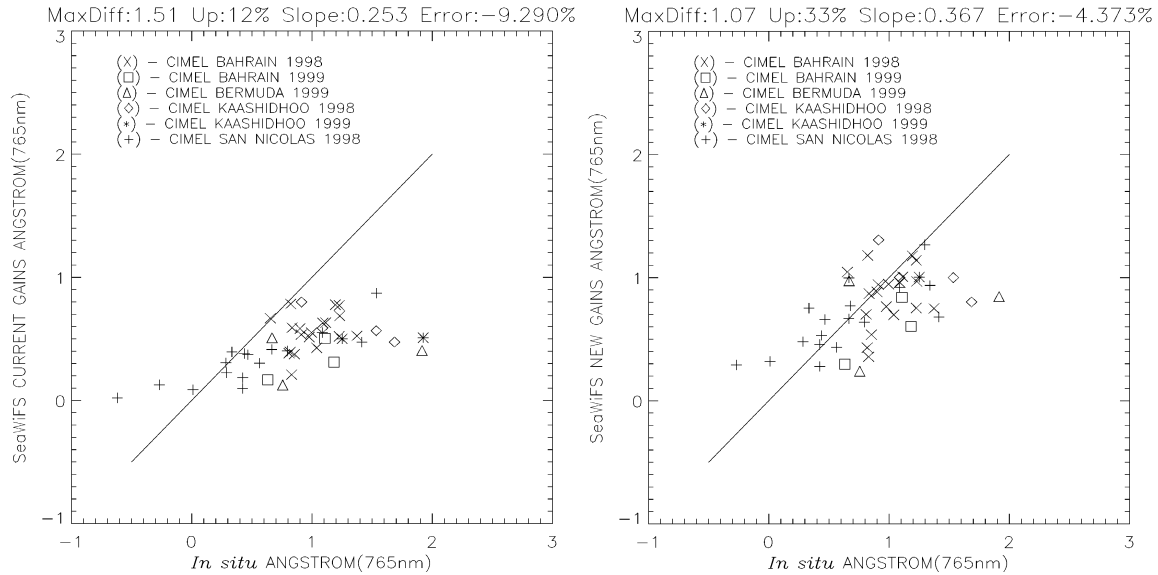


Figure 4: Comparison of aerosol Ångström coefficients in the 765nm band relative to the 865nm band for the AOT match-up points and the operational and alternative set of SeaWiFS calibration gains.

Figure 4 illustrates Ångström coefficient match-ups computed for the 765nm band relative to the 865nm band, which are the bands used to select an aerosol model in the SeaWiFS processing. The alternative calibration approach forced a number of SeaWiFS AOT measurements to produce Ångström coefficients that more closely approximate the coefficients of *in situ* observations. The inaccuracy of Ångström coefficients computed with the alternative calibration is half of the inaccuracy produced with the operational gains. However, this improvement was not sufficient to produce substantially better AOT match-ups in the visible bands.

The improved AOT match-up results indicate that there are inaccuracies in the relative and absolute calibrations of the SeaWiFS near-infrared bands. However, the spectral shape of existing aerosol models may cause more problems in estimating atmospheric contribution to the signal at the top-of-the-atmosphere than do these calibration errors. It has been noted that SeaWiFS aerosol models commonly have flatter

spectral distributions than those obtained from *in situ* AOT measurements. Because of this, the aerosol path radiance models produce underestimated AOT values when extrapolated from the near-infrared spectra to the SeaWiFS visible bands. Before final conclusions can be drawn, however, additional studies should be performed using a larger set of *in situ* data to confirm these results. These studies may include the use of global aerosol measurements to determine the NIR calibration of SeaWiFS, independent of the MOBY observations. Some enhanced screening of the aerosol measurements may also be necessary, as discussed in Chapter 7 of this document.

## 9.5 Conclusions

We have described a procedure to predict TOA reflectance, and hence calibration gains, from well known atmospheric components and simultaneous measurements of water-leaving radiance and aerosol optical thickness. Relative to the standard SeaWiFS calibration technique, this procedure eliminates the requirements for *a priori* knowledge of the calibration at 865nm, and it does not require an assumption of aerosol type. Instead, we have used the measured aerosol optical thickness to define the aerosol concentration, and we have used the measured Ångström coefficient to characterize the aerosol type.

The major limitation of this approach is that we still must use aerosol models to relate the measured aerosol optical thicknesses to aerosol reflectances, and models may not be accurate or uniquely defined with respect to Ångström coefficient. Model uncertainties can be minimized, however, by selecting sites where historical evidence would suggest that the aerosols are generally homogenous and well characterized by existing models.

The major advantage of incorporating aerosol optical thickness measurements into the calibration process is that we can now derive an independent estimate of the calibration at 765 and 865nm. The results of our preliminary analysis compare well with

a growing body of evidence that the SeaWiFS 865nm channel overestimates the TOA radiance by 4 to 10% [19]. The gains retrieved using this alternative method produce minor changes in the SeaWiFS retrieved water-leaving radiances, but a marked improvement in the SeaWiFS retrieved aerosol optical thickness and Ångström exponent.

### References

- [1] P. Y. Deschamps, M. Herman, and D. Tanre, "Modeling of the atmospheric effects and its application to the remote sensing of ocean color," *Appl. Opt.*, vol. 22, pp. 3751-3758, 1983.
- [2] H. R. Gordon and M. Wang, "Influence of oceanic whitecaps on atmospheric correction of ocean-color sensor," *Appl. Opt.*, vol. 33, pp. 7754-7763, 1994.
- [3] M. Wang, "Atmospheric correction of ocean color sensors: Computing atmospheric diffuse transmittance," *Appl. Opt.*, vol. 38, pp. 451-455, 1999.
- [4] H. R. Gordon and M. Wang, "Retrieval of water-leaving radiance and aerosol optical thickness over the oceans with SeaWiFS: a preliminary algorithm," *Appl. Opt.*, vol. 33, pp. 443-452, 1994.
- [5] K. Ding and H. R. Gordon, "Analysis of the influence of O<sub>2</sub> A-band absorption on atmospheric correction of ocean-color imagery," *Appl. Opt.*, vol. 34, pp. 2068-2080, 1995.
- [6] H. R. Gordon, "Remote sensing of ocean color: a methodology for dealing with broad spectral bands and significant out-of-band response," *Appl. Opt.*, vol. 34, pp. 8363-8374, 1995.
- [7] H. R. Gordon, J. W. Brown, R. H. Evans, "Exact Rayleigh scattering calculations for use with Nimbus 7 Coastal Zone Color Scanner," *Appl. Opt.*, vol. 27, pp. 862-871, 1988.

- [8] R. A. Barnes, R. E. Eplee Jr., W. D. Robinson, G. M. Schmidt, F. S. Patt, S. W. Baily, M. Wang, and C. R. McClain, "The calibration of SeaWiFS on orbit," *proc. SPIE*, 31 July – 4 August, 2000.
- [9] D. K. Clark, H. R. Gordon, K. K. Voss, Y. Ge, W. Brokenow, and C. Trees, "Validation of atmospheric correction over oceans," *J. Geophys. Res.*, vol. 102, pp. 17209-17217, 1997.
- [10] D. A. Siegel, M. Wang, S. Moretorena, and W. Robinson, "Atmospheric correction of satellite ocean color imagery: the black pixel assumption," *Appl. Opt.*, vol. 39 no. 21, pp. 3582-3591, 2000.
- [11] S. W. Bailey, C. R. McClain, P. Jeremy Werdell, and Brian D. Schieber, 2000: "Normalized Water-Leaving Radiance and Chlorophyll a Match-up Analyses." In: McClain, C. R., R. A. Barnes, R. E. Eplee, Jr., B. A. Franz, N. C. Hsu, F. S. Patt, C. M. Pietras, W. D. Robinson, B. D. Schieber, G. M. Schmidt, M. Wang, S. W. Bailey, and P. J. Werdell, SeaWiFS Postlaunch Calibration and Validation Analyses, Part 2. NASA Tech. Memo. 2000-206892, Vol. 10, S. B. Hooker and E. R. Firestone, Eds., NASA Space Flight Center, Greenbelt, Maryland, 45 - 52.
- [12] B. N. Holben, T. F. Eck, I. Slutsker, D. Tanre, J. P. Buis, A. Setzer, E. Vermote, J. A. Reagan, Y. Kaufman, T. Nakajima, F. Lavenue, I. Jankowiak, and A. Smirnov 1998: "AERONET - A federated instrument network and data archive for aerosol characterization", *Rem. Sens. Environ.*, 66, 1-16.
- [13] B. N. Holben, D. Tanre, A. Smirnov, T. F. Eck, I. Slutsker, N. Abuhassan, W. W. Newcomb, J. Schafer, B. Chatenet, F. Lavenue, Y. J. Kaufman, J. Vande Castle, A. Setzer, B. Markham, D. Clark, R. Frouin, R. Halthore, A. Karnieli, N. T. O'Neill, C. Pietras, R. T. Pinker, K. Voss, G. Zibordi, 2000: "An emerging ground-based aerosol climatology: Aerosol Optical Depth from AERONET", *J. Geophys. Res.*, In press.

- [14] M. Wang, S. Bailey, C. Pietras, C. R. McClain, and T. Riley, 2000, "SeaWiFS Aerosol Optical Thickness Match-up Analysis", NASA Tech. Memo. 2000-206892, In C. R. McClain, R. A. Barnes, R. E. Eplee, Jr., B. A. Franz, C. H. Hsu, F. S. Patt, C. M. Pietras, W. D. Robinson, B. D. Schieber, G. M. Schmidt, M. Wang, S. W. Bailey, and P. J. Werdell, SeaWiFS Postlaunch Calibration and Validation Analyses, Part 2, S. B. Hooker and E. R. Firestone, Eds, NASA Goddard Space Flight Center, Greenbelt, Maryland.
- [15] W. D. Robinson and M. Wang, "Vicarious Calibration of SeaWiFS Band 7", NASA Tech. Memo. 2000-206892, In C. R. McClain, E. J. Ainsworth, R. A. Barnes, R. E. Eplee, Jr., F. S. Patt, W. D. Robinson, M. Wang, and S. W. Bailey, SeaWiFS Postlaunch Calibration and Validation Analyses, Part 1, S. B. Hooker and E. R. Firestone, Eds, NASA Goddard Space Flight Center, Greenbelt, Maryland.
- [16] R. E. Eplee, Jr., C. R. McClain, "MOBY Data Analysis for the Vicarious Calibration of SeaWiFS Bands 1-6", NASA Tech. Memo. 2000-206892, In McClain, C. R., E. J. Ainsworth, R. A. Barnes, R. E. Eplee, Jr., F. S. Patt, W. D. Robinson, M. Wang, and S. W. Bailey, SeaWiFS Postlaunch Calibration and Validation Analyses, Part 1, S. B. Hooker and E. R. Firestone, Eds, NASA Goddard Space Flight Center, Greenbelt, Maryland.
- [17] C. Cox and W. Munk, "Measurements of roughness of the sea surface from photographs of the Sun's glitter," J, Opt. Soc. Am. 44, 838-850, 1954.
- [18] H. R. Gordon and M. Wang, "Influence of oceanic whitecaps on atmospheric correction of ocean-color sensors," *Appl. Opt.*, Vol. 33, No. 33, pp. 7754-7763, 1994.
- [19] R. A. Barnes, R. E. Eplee, W. D. Robinson, G. M. Schmidt, F. S. Patt, S. W. Bailey, M. Wang, C. R. McClain, "The calibration of SeaWiFS, Proc. 2000

Conf. on Characterization and Radiometric Calibration for Remote Sensing," Logan, Utah, September 19-21, 2000.